JOURNAL OF Materials CHEMISTRY

IR laser-induced thermolysis of (chloromethyl)silane: complex reaction involving H_2Si:, H_2C: and HClSi: transients and yielding nanostructured Si/C/H phases

Josef Pola,*[a] Magna Santos,[b] Luis Díaz,[b] Kristýna Jursíková,[a] Zdeněk Bastl,[c] Jaroslav Boháček,[d] Radek Fajgar[a] and Markéta Urbanová[a]

[a]*Laser Chemistry Group, Institute of Chemical Process Fundamentals, Academy of Sciences of the Czech Republic, 16502 Prague, Czech Republic*
[b]*Instituto de Estructura de la Materia, C. S.I. C., Serrano 121, 28006 Madrid, Spain*
[c]*J. Heyrovský Institute of Physical Chemistry, Academy of Sciences of the Czech Republic, Prague 18223, Czech Republic*
[d]*Institute of Inorganic Chemistry, Academy of Sciences of the Czech Republic, 25068 Řež near Prague, Czech Republic*

Received 3rd January 2002, Accepted 19th February 2002
First published as an Advance Article on the web 22nd March 2002

Multi-pulse and single-pulse infrared laser induced thermolysis of gaseous (chloromethyl)silane, H_3SiCH_2Cl occurs *via* 1,1-HCl and H_2C**:** elimination and dehydrogenation and yields nano-structured Si/C/H phases containing most of the Si and C atoms of the precursor. The identification of final volatile products and observation of H_2Si:, H_2C**:** and HClSi**:** transients by LIF spectroscopy suggest that intermediate silene isomers decompose into silylene and carbene. The deposited films are composed of SiC and polycarbosilane and their H content differs depending on the mode of the IR thermolysis.

Introduction

There is continuing interest[1] in chemical vapour deposition (CVD) of hydrogenated silicon carbide due to the applications of this material in microelectronics, photoelectronics and high-temperature ceramics. Properties of the Si/C/H phases can be improved by using specially designed hydridocarbosilane precursors that offer better control of the Si/C stoichiometry and lower temperatures of the CVD process.[2] Precursors examined so far were mostly organosilanes $RSiH_3$ (R = alkyl, alkenyl and alkynyl)[2,3] whose mechanism of thermal decomposition was well known.[4]

(Chloroorgano)silanes have attracted only little attention.[5] However, the recently reported formation of nanocrystalline SiC materials from chlorine-containing polycarbosilane precursors[6] suggests the potential use of chloroorganosilicon compounds as a source of Si/C/H phases and advocates investigation on thermal decomposition of these compounds.

In a continuation of our studies on laser-induced CVD of organosilanes[7] and on thermal decomposition of gaseous (chloromethyl)trimethylsilane,[8] we present here our results on IR laser-induced thermolysis of (chloromethyl)silane, ClH_2CSiH_3 (CMS) and show this reaction to be dominated by 1,1-HCl elimination and dehydrogenation, and yielding nano-structured Si/C/H phases with low Cl content.

Experimental

Laser thermolysis

Both infrared laser multi-photon decomposition[9] (IRMPD) and laser-powered homogeneous (SF_6-photosensitized) decomposition[10] (LPHD) of CMS was explored. These experiments were performed with a transversely excited atmospheric (TEA) CO_2 laser (Plovdiv University) operating at the P(20) line of the 0001 → 1000 transition (944.2 cm^{-1}). The wavelength and fluence were checked by a model 16-A spectrum analyzer (Optical Eng. Co.) and by a pyroelectric detector (ml-1 JU, Charles University). Gaseous samples of CMS (5–50 Torr) were irradiated in a Pyrex vessel (45 mm id, 10 cm length) equipped with two NaCl windows using laser fluence of 0.2–0.4 J cm^{-2}; samples of ClH_2SiD_3 isotopomer (CMS-d_3, 5 Torr) were irradiated in a mixture with SF_6 (7–10 Torr) sensitizer in a stainless steel cell equipped with Ge windows using fluence of 0.2 J cm^{-2}. In some irradiations, the laser beam was focused with a NaCl lens (focal length 8 cm). Both reactors were furnished with a valve and a sleeve with rubber septum.

Changes in the composition of the irradiated CMS or CMS-d_3 were monitored by an FTIR (Nicolet, model Impact 400) spectrometer. The depletion of CMS and CMS-d_3 was followed by using a diagnostic band at 2173 cm^{-1} and 1567 cm^{-1}, respectively. GC/MS and GC analyses of the gaseous samples after the irradiation were performed on a Shimadzu QP 1000 mass spectrometer and a Shimadzu 14A chromatograph with FID detector which was coupled with a Chromatopac C-R5A computing integrator. Both instruments were equipped with Porapak P and SE-30) columns using programmed temperatures (20–150 °C) and helium carrier gas. The quantitative GC analyses are based on the knowledge of response factors for the identified products that were determined or taken from ref. 11. Hydrogen was determined by using a Balcers QMG 420 mass spectrometer.

Laser induced fluorescence

Real time studies on the fragments produced in the IRMPD of CMS were carried out using a Lumonics K-103 TEA CO_2 laser tuned at the P(10) line of the 0001 → 1000 transition (933 cm^{-1}) . The laser was equipped with a frontal Ge multi-mode optics (35% reflection) and a rear diffraction grating with 135 lines mm^{-1} blazed at 10.6 μm.

The photolysis experiments were performed under gas-flow conditions in cells (12 or 25 cm long) fitted with a pair of NaCl windows orthogonal to another pair of quartz windows. The

DOI: 10.1039/b200061j

CO_2 laser beam was focused at the centre of the reaction cells by NaCl lenses of 10 or 24 cm focal lengths. The sample pressure in the gas flow cell (0.22 Torr) was measured with an MKS Baratron gauge (0–7.5 Torr) and the rate of the CO_2 pulsing was chosen so that a new fresh sample was irradiated with each shot.

Fluorescence was induced in the formed fragments by means of a N_2-pumped dye laser (PRA LN107) with a bandwidth of 1.6 cm^{-1} at 500 nm. The N_2 laser beam was counter-propagating to the CO_2 laser beam and focused by a quartz lens (focal length 50 cm) at the focus of the infrared beam. The relative energy of the dye laser was controlled with a Thorlabs high-speed silicon detector.

The laser induced fluorescence (LIF) experiments with CMS were carried out in three spectral regions by using three different dyes: coumarin 440 and 485 for the 420–475 nm and 480–510 nm region, respectively and rhodamine 590 for the 575–600 nm region. With the two first regions the induced fluorescence was filtered through a 10 cm monochromator and 2 mm slit (bandpass of 6.4 nm). Much weaker signals observed in the third region meant that the whole deexcitation signal was filtered through a 610 cutoff filter instead. The filtered signal was detected in all cases using a R928 Hamamatsu photomultiplier fed with 800 or 1000 V.

The LIF experiments in the 575–600 nm region were also performed to examine IRMPD fragments of 1,3-disilacyclobutane (DCSB), for which purpose the TEA CO_2 laser was tuned at the R(18) line of the 0001 $\rightarrow$ 1000 transition (974.6 cm^{-1}).

The CO_2 laser pulse, picked up with the photon drag detector, triggers a Tektronix TDS 540 digital oscilloscope used to collect the signals and send them to a personal computer where they are averaged and analyzed. The delay between the CO_2 and probe laser pulses ($\sim$1 μs $\pm$ 100 ns) was controlled by a Berkeley Nucleonic BNC 7036A. The CO_2 laser fluence was calculated as the ratio of the pulse energy (measured with a Lumonics 20D pyroelectric detector) and the FWHM cross-sectional beam area (measured at the cell position with a pyroelectric array Delta Development Mark IV). The fluences achieved using the 10 or 24 cm focal length lenses were in the range of 40–50 J cm^{-2}. Lower pressure and fluence (0.04 Torr and 10–12 J cm^{-2}) were used to examine IRMPD of DCSB.

Properties of deposited solids

In order to evaluate the properties of the solid products by FTIR spectroscopy and by X-ray photoelectron spectroscopy (XPS) and by scanning electron microscopy (SEM) and transmission electron microscopy (TEM) techniques, deposits were produced on a sheet of NaCl or copper accommodated in the reactor before irradiation.

XPS measurements were carried out in an ESCA 310 apparatus (Gammadata Scienta, Sweden) with a monochromatized Al Kα source operated at 15 keV and 50 mA. For excitation of Auger Si KLL electrons the bremsstrahlung radiation produced by an unmonochromatized X-ray source was used. The pressure during spectral acquisition was in the 10^{-10} Torr range. The spectra were acquired at a pass energy of 300 eV with the sample surface normal to the analyzer electron optics. High resolution spectral scans were taken over the Si 2p, C 1s, O 1s and Si KLL spectral regions. The spectra were fitted using a Voight function and Shirley background. The samples were measured first as received and then the measurement was repeated after mild sputtering by argon ions (energy of ions 5 keV, ion current 40 μA, 5 min). The elemental surface concentrations were calculated from the spectral intensities corrected for transmission function of the spectrometer and using theoretical values of photoionization cross-sections.

SEM and TEM analysis of the deposits were carried out on an ultrahigh vacuum Tesla BS 350 instrument and a Philips 201 microscope, respectively.

CMS was prepared by reducing (chloromethyl)trichlorosilane by lithium aluminium hydride in di-*n*-butyl ether as reported[12] and CMS-d_3 was obtained by the same procedure using lithium aluminium deuteride. The purity of both compounds (better than 95%) was checked by GC and FTIR spectroscopy. Their mass spectra were taken with the Shimadzu QP 1000 mass spectrometer operating at an ionizing voltage 70 eV.

Results and discussion

Laser thermolysis of CMS

The TEA CO_2 laser irradiation into the $\delta(H_3Si)$ mode of CMS (5–50 Torr) initiates IRMPD of CMS and yields gaseous products along with a solid material that is deposited onto the cell surface. This decomposition occurs as a non-explosive multi-pulse, or as an explosive single-pulse reaction. The single-pulse IRMPD is achieved with pressures as low as 15 Torr using focused radiation. The non-focused radiation initiates multi-pulse IRMPD that is enhanced with increasing pressure when comparable decomposition progress is accomplished with lower number of pulses. This is in line with collisionally assisted IRMPD as also observed with *e.g.* silane (ref. 13). The pressure increase up to 50 Torr results in IRMPD initiated by just a single pulse and resulting in 75% depletion of CMS (Table 1).

The gaseous products are hydrogen chloride, methane, ethene, ethane, methylsilane and hydrogen (Table 1) that are accompanied with traces of dimethylsilane and butane. The high yields of HCl and H_2 and very low yields of the hydrocarbons are in keeping with C and Si atoms being efficiently utilized in the formation of the solid deposit and with Cl being mostly liberated into the gas phase. These volatile products also reveal that the CMS decomposes *via* expulsion of HCl and H_2 yielding unsaturated transient(s) that undergo polymerization and form the solid material.

The major decomposition modes of organosilanes $RSiH_3$ are[4] 1,1-H_2, 1,2-H_2 and 1,2-hydrocarbon eliminations; these steps and HCl elimination make the possible reaction scheme rather complex (Scheme 1). However, some suggested steps will be judged to be less important than others.

The irradiation of CMS-d_3 in the presence of SF_6 sensitizer helped in understanding the mode of HCl formation. LPHD of the d_3-isotopomer yields the same relative amounts of the gaseous hydrocarbons. The FTIR spectral analysis (Fig. 1)

Table 1 Typical runs of IRMPD of CMS

Run	CMS/ Torr	Fluence/ J cm^{-2}	No. of pulses	Decomp. progress (%)	Yield of gaseous products[a]					
					CH_4	C_2H_4	C_2H_6	CH_3SiH_3	H_2	HCl
1	10	0.40	35	41	5	5	3	5	21	70
2	15	0.30	20	47	3	3	3	4–5	28	85
3	50	0.20	1	75	1	3	–	2	37	>75
4[b]	15	0.35	1	100	2	<1	1	0		>75

[a]In mole/mole of CMS decomposed $\times$100. [b]Focused radiation.

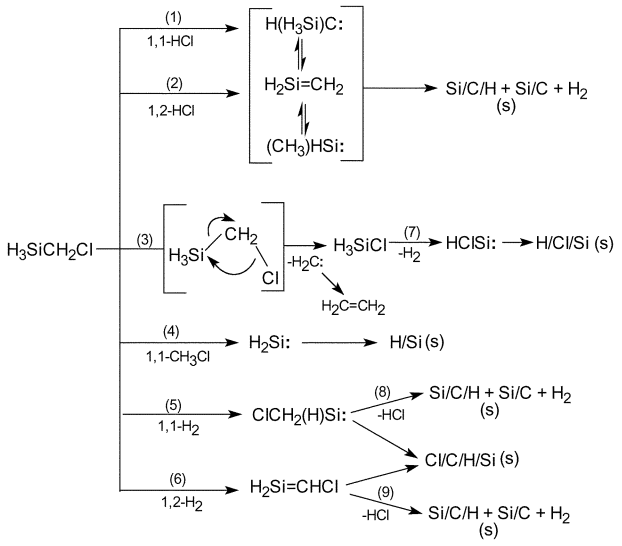

Scheme 1 Possible decomposition pathways of CMS.

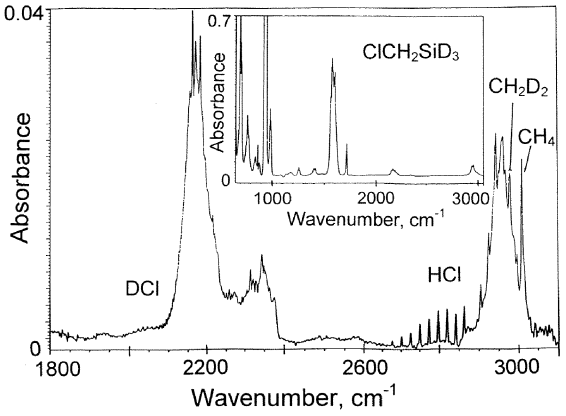

Fig. 1 Part of FTIR spectrum of the irradiated (fluence 0.16 J cm^{-2}, 10^3 pulses) mixture of CMS-d_3-SF_6; Inset: CMS-d_3 (5 Torr)-SF_6 (10 Torr) before irradiation.

reveals[14] the presence of CH_4 (3010 cm^{-1}), CH_2D_2 (2976 cm^{-1}) and possibly of other CH_nD_{4-n} isotopomers. HCl is found to dominate over DCl: in some runs only HCl and in others HCl accompanied by only very small amounts of DCl was observed. This indicates that step (2) is insignificant. Step (4) can be also considered to be insignificant, because CH_3Cl was not detected among the products and chloromethane thermolysis occurring[15] *via* a radical mechanism and involving Cl atoms would have produced a mixture of significant amounts of DCl and HCl.

Formation of H_2 can be due to dehydrogenation of the transients produced by step (1), dehydrogenation of H_3SiCl [step (3)], and/or dehydrogenation of CMS [step (5) and (6)].

The 1,2-Cl shift and methylene [step (3)] was observed[16] with similar compound, $(CH_3)_3SiCH_2Cl$ and would yield H_3SiCl (ref. 17) which was not detected among the products. However, chlorosilane is known[18] to decompose *via* a dehydrogenation [step (7)] into chlorosilylene. The fact that both methylene and chlorosilylene were detected by the LIF analysis (see later) shows that the sequence of steps (3) and (7) is plausible.

The dehydrogenation steps (5) and (6) yield chlorinated unsaturates that would polymerize and produce polychlorocarbosilanes,[19] or split HCl and form highly reactive $SiCH_2$ transients polymerizing[20] into polycarbosilanes. The latter route is probable, since the solid product is very poor in Cl (see later). That the three-centre HCl elimination[21] is considerably faster than 1,1- and 1,2-elimination of H_2 (and this is so in the

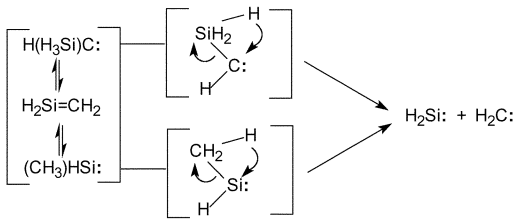

Scheme 2 Decomposition of $SiCH_4$ transients.

temperature range 600–1000 K)[4d] makes us, however, believe that step (1) is more likely than steps (5) and (6).

We can thus judge that the major routes of the IRMPD of CMS are two routes that are (a) isomerization of silylcarbene[22] and dehydrogenation of the $SiCH_4$ transients [initiated by step (1)], and (b) elimination of carbene and dehydrogenation of chlorosilane [steps (3) and (7)]. We assume that CO_2 laser radiation is efficiently absorbed by $H_2Si{=}CH_2$ (ref. 23), $H(H_3Si)C$**:** and H_3SiCl transients, which enables excitation of these species once they are generated and induces their dehydrogenation. Another route of the $SiCH_4$ transients can be their decomposition into H_2C**:** and H_2Si**:** species that were proved by the LIF experiments (see later). This as yet unobserved expulsion of silylene from silylmethylene, and that of methylene from methylsilylene, is illustrated in Scheme 2. To distinguish between these paths through scavenging of intermediary silylenes or silenes is in these experiments typically[24] not an easy task; these inferences therefore rely on the decomposition of CMS-d_3 and on the LIF experiments.

LIF experiments with CMS

The excitation spectra obtained by scanning the dye laser (Fig. 2) reveal several bands in the 420–460 nm and 490–560 regions. These were assigned[25] to the $\Delta v = 4$ and 3 and $\Delta v = 1$ and 2 ($\tilde{A}\,^1A'' \leftarrow \tilde{X}\,^1A'$) transitions of the v_2 mode of the HClSi**:** fragment. These assignments have been verified by obtaining the dispersion spectra of the three excitation bands in the first region and of the bands corresponding to the transitions (0,1,0) $\rightarrow$ (0,0,0) and (0,5,0) $\rightarrow$ (0,3,0) in the second region.

The excitation spectrum obtained for the 575–600 nm region (Fig. 3) presents two broad unstructured bands centred at 578.5 and 585 nm that can be assigned[26] to the ($\tilde{A}\,^1B_1 \leftarrow \tilde{X}\,^1A_1$) (0,2,0) $\leftarrow$ (0,0,0) and (0,3,0) $\leftarrow$ (0,1,0) transitions of the H_2Si**:** fragment. The width and lack of structure of these bands suggest a high content of internal excitation in the formed H_2Si**:**

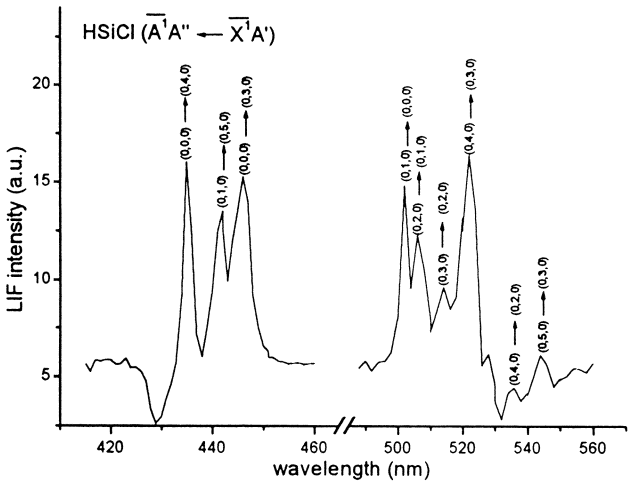

Fig. 2 LIF excitation spectra following IRMPD of CMS showing the ($\tilde{A}\,^1A'' \leftarrow \tilde{X}\,^1A'$) transitions of the v_2 mode of the HClSi**:** fragment.

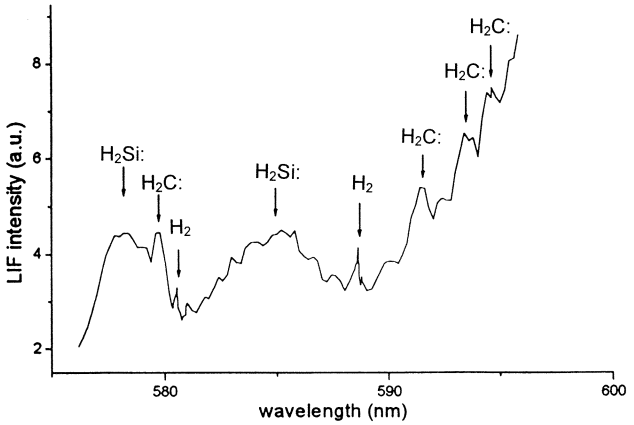

Fig. 3 LIF excitation spectra following IRMPD of CMS showing bands belonging to the H_2Si:, H_2C: and H_2 fragments. The corresponding assignments are given in the text.

fragments. There are also some narrower and weaker bands centred at 579.8, 591.4, 593.4 and 594.4 nm. We assign[27] the first of them to the (0,16,0) ← (0,1,0) transition of H_2C: and the others to the (0,14,0) ← (0,0,0) transitions of H_2C: fragment. Finally, the weak but sharp bands centred at 580.5 and 588.6 nm correspond[28] to molecular H_2.

LIF experiments with DSCB

These experiments were performed to help the identification of the dissociation paths taking place in the IRMPD of CMS. The IRMPD[2e,29] (and also conventional thermolysis[30]) of DSCB is considered to yield transient silene (Scheme 3) and could thus provide strong support for the proposed decomposition of the $SiCH_4$ transients into silylene and carbene (Scheme 2). Indeed, the LIF experiments on IRMPD of DSCB carried out in the 575–600 nm spectral region revealed[31] the occurrence of H_2Si:, H_2C: (and also H_2). A more structured profile of the obtained excitation spectrum suggests that these species are poorer in rotational/vibrational energy than when they are produced from CMS.

Fragmentation of CMS and CMS-d_3 under electron impact

Common similarities between thermal and electron-impact fragmentation of many organic molecules spurred us to examine mass spectra of CMS and its d_3-isotopomer.

The mass spectrum of CMS [*m/z* (relative intensity > 10%) = 81 (21), 79 (53), 67 (29), 65 (100), 63 (74), 45 (11), 44 (28), 43 (95), 42 (30), 41 (17), 31 (21), 29 (20), 28 (30)] is consistent with the two major signals; that at *m/z* 65 is assignable to $SiH_2{}^{35}Cl^+$ or $Si^{37}Cl^+$ and that at 43 to $HSiCH_2{}^+$ (see also ref. 32). The mass spectrum of CSM-d_3 [*m/z* (relative intensity > 10%) = 83 (44), 81 (65), 69 (35), 67 (100), 65 (32), 63 (77), 46 (23), 45 (37), 44 (28)] allows assignment of the signal at *m/z* 69 to $SiD_2{}^{37}Cl^+$ and that at *m/z* 67 to $SiD_2{}^{35}Cl^+$. These fragments reveal expulsion of CH_2 and a (C)Cl → (Si)Cl rearrangement. The less significant fragments belonging to M − (H, HCl) and M − (D, HCl) at *m/z* 43 and 45 can arise from the split of H (D) and 1,1-HCl elimination.

The fragmentation under electron impact of both isotopomers thus reveals that expulsion of CH_2 (CD_2) is more

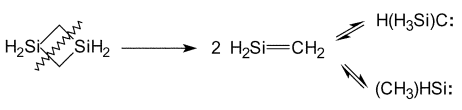

Scheme 3 Decomposition of DSCB.

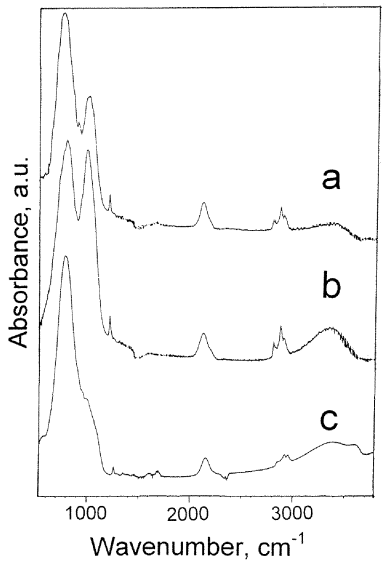

Fig. 4 Typical FTIR spectra of the deposits from multi-pulse IRMPD (a), from multi-pulse IRMPD when exposed to air (b) and from single-pulse IRMPD (c, Run 4 in Table 1).

important. This fragmentation mode is in keeping with step (3) in Scheme 1.

Properties of the solid deposits

FTIR spectra of the deposits show a pattern typical of polycarbosilanes which is little affected by irradiation conditions. The absorption bands of the deposit obtained by the multi-pulse and the single-pulse IRMPD (Fig. 4) can be assigned as in Table 2. Both spectra consist of contributions due to *ν*(Si–C), *δ*(CH_3Si), *ν*(Si–H) and *ν*(C–H) vibrations. The absorbance at the *ν*(Si–H) and *ν*(C–H) vibrations is indicative[33,34] of the distribution of H atoms between Si and C centers. The A*ν*(C–H) : A*ν*(Si–H) ratio in the deposits from the multi-pulse IRMPD being ~1 is in keeping with roughly 5 times higher concentration of the H(C) centers, whereas that in the deposits from the single-pulse IRMPD (~0.4) shows *ca.* twofold excess of H(C) over H(Si) centers. FTIR spectra of the deposits reveal formation of *ν*(Si–O) and *ν*(OH) absorption bands upon exposure to air (Fig. 4b). These changes reflect[35,36] the reaction of air moisture and/or oxygen with naked Si atoms or Si=C bonds] and/or a well-known reaction of air moisture with some residual Si–Cl bonds which are produced during the deposition process.

Additional information on the chemistry of the deposited material is obtained from the XPS measurements. The surface composition of the deposits calculated from intensities of the Si 2p, C 1s, O 1s and Cl 2p photoemission lines—$Si_{1.00}C_{0.73}O_{1.29}$ for the explosive IRMPD and $Si_{1.00}C_{1.02}O_{1.00-1.15}Cl_{0.10-0.20}$ for the non-explosive IRMPD—shows incorporation of oxygen

Table 2 Typical FTIR spectra of the Si/C/H deposits[a]

	Wavenumber/cm^{-1} (absorptivity)[b]		
Vibrational mode	I	II	III
ν(Si–C)	833 (1.00)	833 (1.00)	820 (1.00)
ν(Si–O)	1064 (0.62)	1039 (0.93)	–
δ(CH_3Si)	1263 (0.07)	1263 (0.07)	1255 (0.03)
ν(Si–H)	2169 (0.12)	2169 (0.11)	2151 (0.08)
ν(C–H)	2927 (0.11)	2927 (0.12)	2925 (0.03)

[a]I, II and III designate, in the given order, typical deposit from the multi-pulse IRMPD , that from the multi-pulse IRMPD exposed to air, and that from the explosive single/pulse IRMPD (Run 4). [b]Normalized to that of the *ν*(Si–C) band.

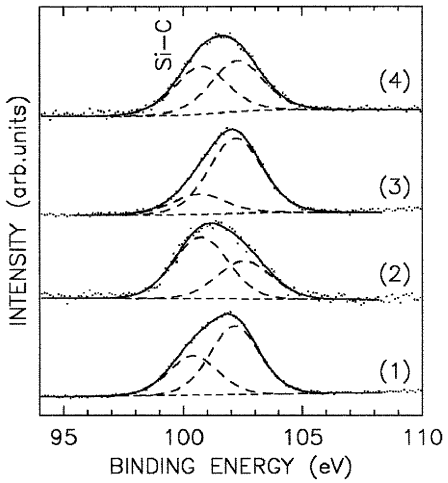

Fig. 5 Si (2p) core level spectra of the deposit from multi-pulse (1) and single-pulse (3) IRMPD (Run 3, Table 1) and of the corresponding deposits sputtered with Ar ions (2 and 4, respectively).

and chlorine. The different content of Cl in both deposits must be related to the fact that the chlorinated unsaturated transients (Scheme 1) undergo some polymerization in the non-explosive IRMPD and that they eliminate HCl before they polymerize in the explosive IRMPD. The Si 2p core level spectrum (Fig. 5) is best fitted by two components, one belonging to SiC and located at 100.3 eV and another one centered at 102.3 eV assignable[37] to an Si–O bond. The presence of silicon carbide in the deposits is consistent with the obtained value of the Auger parameter, 1714.7 eV, and is further supported by the presence of the carbidic component in the spectra of C 1s electrons (Fig. 6). The argon ion sputtering leads to the increase of the carbidic component in the Si 2p spectra (Fig. 5) and the decrease of the surface concentration of oxygen by 36–50%. These findings reveal that oxygen incorporation into superficial layers takes place during transport of the samples from the reactor to the spectrometer chamber and is due to superficial oxidation and/or hydrolysis of the Si–Cl bonds.

SEM images of the deposits obtained by the single- and multi-pulse IRMPD show similar morphology that is represented by a woven texture (Fig. 7). TEM analysis (Fig. 8) reveals that both types of deposits are chain-like structures of agglomerates whose size depends on the irradiating conditions and is *ca.* 10 nm (the single-pulse IRMPD) or *ca.* 50 nm (the multi-pulse IRMPD).

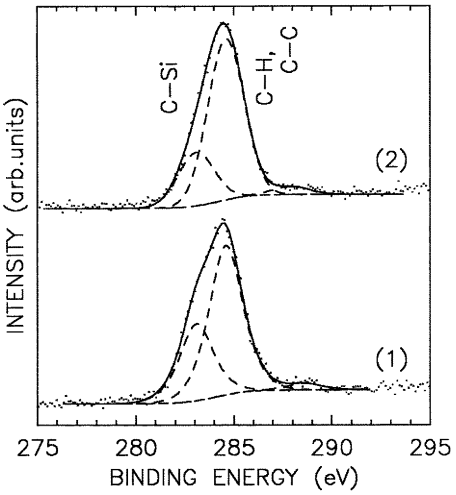

Fig. 6 C (1s) core level spectra of the deposit from multi-pulse (1) and single pulse (Run 3, Table 1) IRMPD.

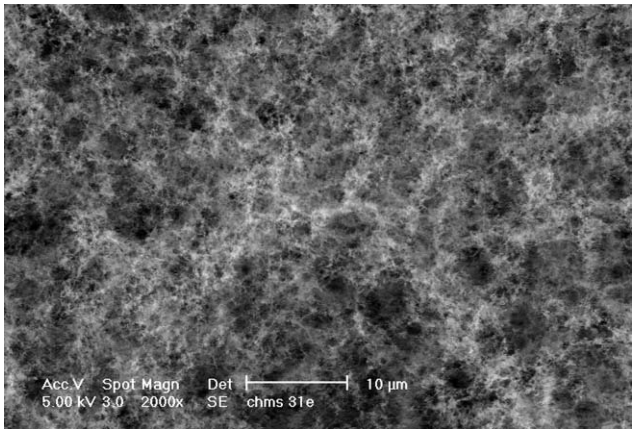

Fig. 7 SEM of the deposit from multi-pulse IRMPD of CMS.

Conclusions

CMS undergoes single-pulse and multi-pulse IRMPD to yield HCl and H_2 as major and methane, ethane, ethane and methylsilane as very minor gaseous products. The Si and C atoms of CMS are efficiently used for the formation of the solid nano-structured polycarbosilane films that arise by a multitude of reactions. These involve initial 1,1-HCl and H_2C**:** elimination from CMS and decomposition and dehydrogenation of $SiCH_4$ (silene, methylsilylene and silylmethylene) transients.

The three-centre elimination of HCl differs from thermal

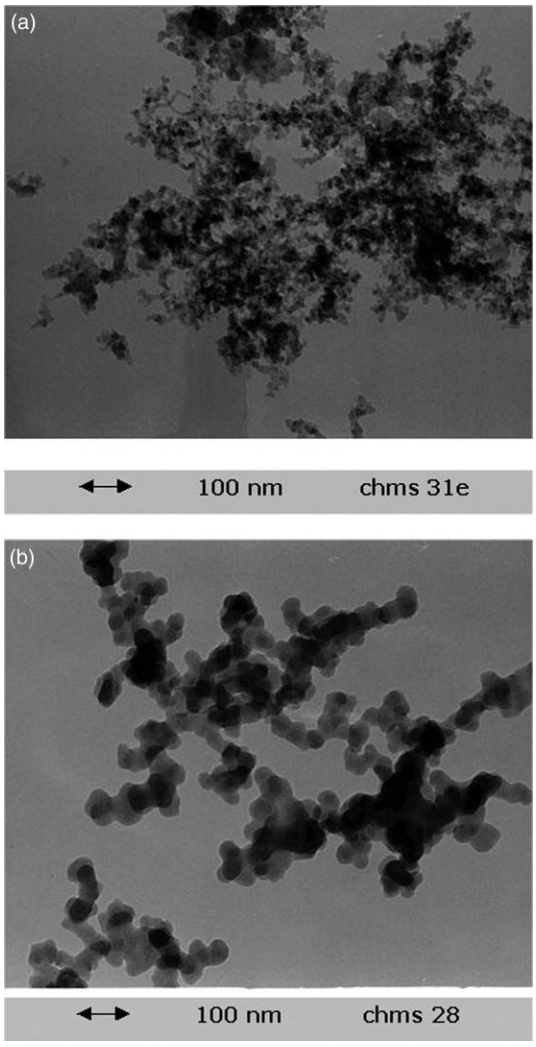

Fig. 8 TEM of the deposit from single-pulse (a) and multi-pulse (b) IRMPD of CMS.

decomposition of other carbon-functional organosilicon compounds $R_nX_{3-n}Si(CH_2)_mY$ (R = alkyl, X, Y = electronegative moiety) which is controlled[38] by intramolecular Si → Y interactions in the transition state and yields[8,39] with (halogenomethyl)silanes $R_nX_{3-n}SiCH_2$–Z (Z = halogen) products with the Si–Z bond.

The nano-structured polycarbosilane films are composed of SiC and polycarbosilane and their hydrogen content is lower when produced from explosive single-pulse IRMPD. They incorporate oxygen in superficial layers upon contact with air.

Acknowledgement

The work was supported by the Grant Agency of the Czech Republic (grant no. 104/00/1294) and by the Spanish Dirección General de Investigación (MCyT) (BQU2000-1163-C02-02). The authors thank Drs A. Galík and A. Galíková for analysis of hydrogen.

References

1 *e.g.* (*a*) L. Jiang, X. Chen, X. Wang, L. Xu, F. Stubhan and K.-H. Merkel, *Thin Solid Films*, 1999, **352**, 97 and refs. therein; (*b*) J. M. Agullo, F. Fau-Canillac and F. Maury, *J. Mater. Chem.*, 1994, **4**, 695; (*c*) A. E. Kaloyeras, J. W. Corbett, P. J. Toscano and R. B. Rizk, *Mater. Res. Symp. Proc.*, 1990, **192**, 601.

2 *e.g.* (*a*) J. Pola, J. Vitek, Z. Bastl, R. Fajgar, S. Graschy and K. Hassler, *Main Group Met. Chem.*, 1999, **22**, 545 and refs. therein; (*b*) A. D. Johnson, J. Perrin, J. A. Mucha and D. E. Ibbotson, *J. Phys. Chem.*, 1993, **97**, 12937; (*c*) V. M. Scholz, W. Fuss and K.-L. Kompa, *Adv. Mater.*, 1993, **5**, 38; (*d*) E. A. Volnina, J. Kupčík, Z. Bastl, J. Šubrt, L. E. Guselnikov and J. Pola, *J. Mater. Chem.*, 1997, **7**, 637; (*e*) Z. Bastl, H. Bürger, R. Fajgar, D. Pokorná, J. Pola, M. Senzlober, J. Šubrt and M. Urbanová, *Appl. Organometl. Chem.*, 1996, **10**, 83.

3 *e.g.* (*a*) J. Pola, Z. Bastl, J. Šubrt and R. Taylor, *J. Mater. Chem.*, 1995, **5**, 1345; (*b*) J. Pola, Z. Bastl, J. Šubrt, J. R. Abeysinghe and R. Taylor, *J. Mater. Chem.*, 1996, **6**, 155; (*c*) J. Pola, J. Vítek, Z. Bastl, M. Urbanová, J. Šubrt and R. Taylor, *J. Mater. Chem.*, 1997, **7**, 1415.

4 (*a*) M. A. Ring and H. E. O'Neal, *J. Phys. Chem.*, 1992, **96**, 10848; (*b*) C. C. Newman, H. E. O'Neal, M. A. Ring, F. Leska and N. Shipley, *Int. J. Chem. Kinet.*, 1979, **11**, 1167; (*c*) S. F. Rickborn, M. A. Ring and H. E. O'Neal, *Int. J. Chem. Kinet.*, 1984, **16**, 1371; (*d*) M. A. Ring, H. E. O'Neal, S. F. Rickborn and B. A. Sawrey, *Organometallics*, 1983, **2**, 1891.

5 (*a*) J. A. O'Neill, M. Horsburgh, J. Tann, K. J. Grant and G. L. Paul, *J. Am. Ceram. Soc.*, 1989, **72**, 1130; (*b*) M. Santos, L. Díaz, Z. Bastl, V. Hulínský, M. Urbanová, J. Vítek and J. Pola, *J. Mater. Chem.*, 1996, **6**, 975.

6 B. S. Mitchell, H. Zhang, M. Ade, D. Kurtenbach and E. Müller, *Mater. Res. Soc. Symp. Proc.*, 2000, **581**, 205.

7 (*a*) J. Pola, *Res. Chem. Intermed.*, 1999, **25**, 351 and refs. therein; (*b*) J. Pola, A. Ouchi, M. Urbanová, Y. Koga, Z. Bastl and J. Šubrt, *J. Organomet. Chem.*, 1999, **575**, 246.

8 M. Urbanová and J. Pola, *J. Anal. Appl. Pyrol.*, 2001, **62**, 197.

9 (*a*) V. S. Letokhov, *Nonlinear Laser Chemistry, Multi-photon Excitation*, Springer-Verlag, Berlin, 1983; (*b*) W. C. Danen and J. C. Jang, in *Laser-Induced Chemical Processes*, ed. J. I. Steinfeld, Plenum Press, New York, 1981.

10 (*a*) W. M. Shaub and S. H. Bauer, *Int. J. Chem. Kinet.*, 1975, **7**, 509; (*b*) D. K. Russell, *Chem.Soc. Rev.*, 1990, **19**, 407; (*c*) J. Pola, *Spectrochim. Acta Part A*, 1990, **46**, 607.

11 W. A. Dietz, *J. Gas Chromatogr.*, 1967, **49**, 151.

12 H. D. Kaesz and F. G. A. Stone, *J. Chem. Soc.*, 1957, 1433.

13 T. F. Deutsch, *J. Chem. Phys.*, 1979, **70**, 1187.

14 S. Pinchas and I. Laulicht, *Infrared spectra of labelled compounds*, Academic Press, London, 1971.

15 E. S. Swinbourne, in *Comprehensive Chemical Kinetics*, eds. C. H. Bamford, C. F. H. Tipper, Vol. 5, Ch. 2, Elsevier, Amsterdam, 1972.

16 M. Urbanová and J. Pola, *J. Anal. Appl. Pyrol.*, 2001, **62**, 197.

17 C. Newman, J. K. O'Loane, S. R. Polo and M. K. Wilson, *J. Chem. Phys.*, 1956, **25**, 855.

18 K. L. Walker, R. E. Jardine, M. A. Ring and H. E. O'Neal, *Int. J. Chem. Kinet.*, 1998, **30**, 69.

19 M. Jakoubková, R. Fajgar, J. Tláskal and J. Pola, *J. Organomet. Chem.*, 1994, **466**, 29.

20 (*a*) J. Pola, *Res. Chem. Intermed.*, 1999, **25**, 351; (*b*) J. Pola, *Surf. Coat. Technol.*, 1998, **100–101**, 408.

21 S. W. Benson and H. E. O'Neal, *Kinetic Data on Gas Phase Unimolecular Reactions*, National Bureau of Standards (USA), 1970.

22 G. Raabe and J. Michl, in *The Chemistry of Organic Silicon Compounds*, eds. S. Patai and Z. Rappoport, J. Wiley, Chichester, 1989, Ch. 17.

23 G. Maier, G. Mihm and H. P. Reisenauer, *Angew. Chem., Int. Ed. Engl.*, 1981, **20**, 597.

24 M. T. Swihart and R. W. Carr, *J. Electrochem. Soc.*, 1997, **144**, 4357.

25 M. Castillejo, R. De Nalda, M. Oujja, L. Díaz and M. Santos, *J. Photochem. Photobiol. A: Chem.*, 1997, **110**, 107.

26 (*a*) I. Dubois, *Can. J. Phys.*, 1968, **46**, 2485; (*b*) M. Fukushima, S. Mayama and K. Obi, *J. Chem. Phys.*, 1992, **96**, 44.

27 G. Herzberg and J. W. C. Johns, *Proc. R. Soc. London Ser. A*, 1966, **295**, 107.

28 (*a*) G. Herzberg, *Molecular Spectra and Molecular Structure I. Spectra of Diatomic Molecules*, Van Nostrand, New York, 1950; (*b*) H. G. Gale, G. S. Monk and K. O. Lee, *Astrophys. J.*, 1928, **67**, 89.

29 S. Dhanya, K. Awadhesh, R. K. Vatsa, R. D. Saini, J. P. Mittal and J. Pola, *J. Chem. Soc., Faraday Trans.*, 1996, **92**, 179.

30 (*a*) G. Raabe and J. Michl, *Chem. Rev.*, 1985, **85**, 419; (*b*) S. Bailleux, M. Bogey, J. Demaison, H. Bürger, M. Senzlober, J. Breidung, W. Thiel, R. Fajgar and J. Pola, *J. Chem. Phys.*, 1997, **106**, 10016.

31 M. Santos and L. D. Díaz, unpublished results.

32 J. M. Bellama and A. G. MacDiarmid, *J. Organomet. Chem.*, 1969, **18**, 275.

33 H. C. Low and P. John, *J. Organomet. Chem.*, 1980, **201**, 363 and refs. therein.

34 H. Shanks, C. J. Fung, L. Ley, M. Cardona, F. J. Demond and S. Kalbitzer, *Phys. Status Solidi*, 1980, **100**, 43.

35 M. T. Davidson, C. E. Dean and F. T. Lawrence, *J. Chem. Soc., Chem. Commun.*, 1981, 52.

36 R. West, H. B. Yokelson, G. R. Gilette and A. J. Millevolte, in *Silicon Chemistry*, eds. E. R. Corey, J. Y. Corey and P. P. Gaspar, Horwood, Chichester, 1988, p. 269.

37 (*a*) R. C. Grey, J. C. Carver and D. M. Hercules, *J. Electron Spectrosc. Relat. Phenom.*, 1976, **8**, 343; (*b*) C. D. Wagner, D. E. Passoja, H. F. Hillery, T. G. Kiniski, H. A. Six, W. T. Jansen and J. A. Taylor, *J. Vac. Sci. Technol.*, 1982, **21**, 933; (*c*) NIST X-Ray Photoelectron Spectroscopy Database, Ver. 2.0, NIST, Gaithersburg, 1997.

38 J. Pola, in *Carbon-functional Organosilicon Compounds*, eds. V. Chvalovský and J. M. Bellama, Plenum Press, New York, 1984, Ch. 2.

39 (*a*) A. G. Brook and P. F. Jones, *J. Chem. Soc., Chem. Commun.*, 1969, 1325; (*b*) W. I. Bevan, R. N. Haszeldine, J. Middleton and A. E. Tipping, *J. Organomet. Chem.*, 1970, **23**, C17; (*c*) G. Fishwick, R. N. Haszeldine, C. Parkinson, P. J. Robinson and R. F. Simmons, *J. Chem. Soc., Chem. Commun.*, 1965, 382; (*d*) H. Beckers and H. Bürger, *J. Organomet. Chem.*, 1990, **385**, 207; (*e*) K. G. Sharp and T. D. Coyle, *J. Fluorine Chem.*, 1971, **1**, 249.